

AGMark: Attention-Guided Dynamic Watermarking for Large Vision-Language Models

Yue Li*
 yue_li@stu.ecnu.edu.cn
 East China Normal University
 China, Shanghai

Yongyi Cui
 yy cui@stu.ecnu.edu.cn
 East China Normal University
 China, Shanghai

Xin Yi*
 xinyi@stu.ecnu.edu.cn
 East China Normal University
 China, Shanghai

Gerard de Melo
 gdm@demelo.org
 Hasso Plattner Institute
 University of Potsdam
 Germany, Potsdam

Dongsheng Shi
 dongsheng@stu.ecnu.edu.cn
 East China Normal University
 China, Shanghai

Linlin Wang†
 llwang@cs.ecnu.edu.cn
 East China Normal University
 China, Shanghai

Abstract

Watermarking has emerged as a pivotal solution for content traceability and intellectual property protection in Large Vision-Language Models (LVLMs). However, vision-agnostic watermarks may introduce visually irrelevant tokens and disrupt visual grounding by enforcing indiscriminate pseudo-random biases. Additionally, current vision-specific watermarks rely on a static, one-time estimation of vision critical weights and ignore the weight distribution density when determining the proportion of protected tokens. This design fails to account for dynamic changes in visual dependence during generation and may introduce low-quality tokens in the long tail. To address these challenges, we propose Attention-Guided Dynamic Watermarking (AGMark), a novel framework that embeds detectable signals while strictly preserving visual fidelity. At each decoding step, AGMark first dynamically identifies semantic-critical evidence based on attention weights for visual relevance, together with context-aware coherence cues, resulting in a more adaptive and well-calibrated evidence-weight distribution. It then determines the proportion of semantic-critical tokens by jointly considering uncertainty awareness (token entropy) and evidence calibration (weight density), thereby enabling adaptive vocabulary partitioning to avoid irrelevant tokens. Empirical results confirm that AGMark outperforms conventional methods, observably improving generation quality and yielding particularly strong gains in visual semantic fidelity in the later stages of generation. The framework maintains highly competitive detection accuracy (at least 99.36% AUC) and robust attack resilience (at least 88.61% AUC) without sacrificing inference efficiency, effectively establishing a new standard for reliability-preserving multi-modal watermarking.

CCS Concepts

- Computing methodologies → Computer vision; Natural language processing;
- Security and privacy → Digital rights management.

Keywords

Dynamic, Watermarking, Large Vision-Language Models

1 Introduction

Large vision-language models (LVLMs) demonstrate strong capabilities across a broad spectrum of downstream tasks [17, 31]. However, their increasing deployment also introduces risks of malicious misuse, motivating the need for robust intellectual property protection and reliable mechanisms to ensure content authenticity [16]. Model watermarking addresses this by embedding identifiable signals into generated content for source attribution and traceability [33]. Existing watermarking techniques [22] can be categorized into logits-based and sampling-based methods, and the former has become the dominant line of work [19]. The pioneering method, KGW [11], employs a secret hash key to partition the vocabulary into green and red token sets and biases the generation process toward green tokens. Building on this framework, follow-up studies propose detection statistics based on token entropy [7, 13] or the green-list probability mass [29], aiming to better balance watermark detectability and generation quality.

Most existing watermarking techniques are developed for text-only large language models (LLMs) and do not adequately account for the challenges posed by LVLMs under multi-modal conditioning [22]. Both random vocabulary partitioning (logits-based paradigm) and uniform logit manipulation (sampling-based paradigm) disrupt vision-conditioned language generation by introducing vocabulary biases that contradict actual visual semantics (e.g., objects, scene descriptors). Consequently, naively applying these methods to LVLMs often leads to perceptible degradation in the quality and fidelity of the generated text. Some recently proposed watermarking methods [21, 35] tailored for LVLMs have made promising progress by embedding detectable watermarks while maintaining semantic fidelity: They identify the cross-modal coordination-critical weight for each vocabulary token and protect a selected portion of highly important evidence. However, two fundamental limitations remain: These methods compute vision-critical token weights only once at initialization, and they ignore the guiding role of the density of the weight distribution when determining the proportion of protected tokens. This may cause misalignment in semantic-critical evidence in later stages of generation and, under an overly concentrated weight distribution, introduce low-quality tokens in the long tail. Figure 1 illustrates these shortcomings with a concrete

*Equal Contribution.

†Corresponding Author.

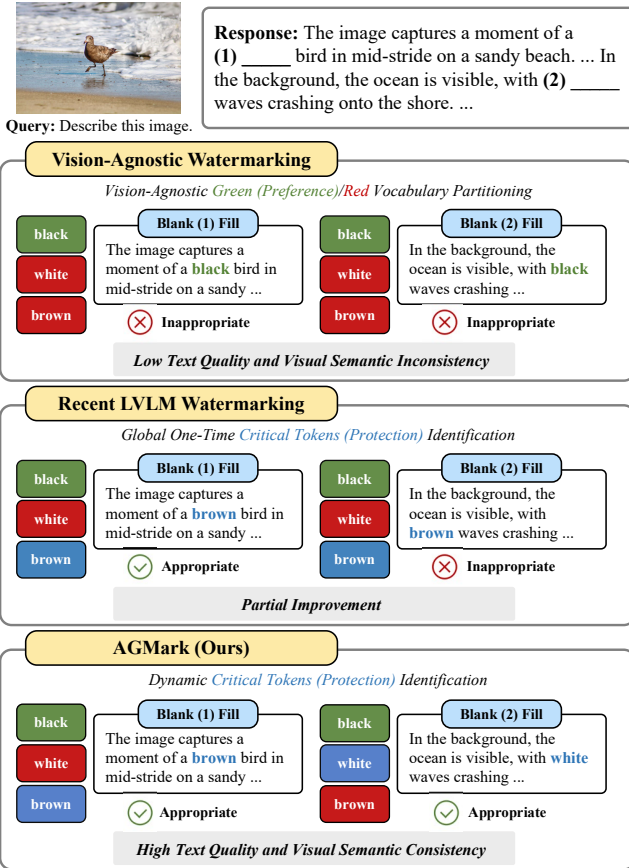


Figure 1: Paradigm comparison of our AGMark, vision-agnostic watermarking methods, and recent LVLM watermarking methods.

example, covering both vision-agnostic watermarking and recent LVLM watermarking methods.

To address these challenges, we propose Attention-Guided Dynamic Watermarking (**AGMark**), a two-stage watermarking framework that dynamically aligns visual semantics and supporting evidence at each decoding step. First, **Semantic Critical Weight Extraction** estimates the current semantic-critical weights by leveraging contextual coherence, and measures real-time reliance on visual semantics using attention weights over visual regions. Second, **Adaptive Vocabulary Partitioning** increases the protected-token proportion under low uncertainty and dispersed evidence weights, thereby ensuring high-quality selection and sufficient coverage of semantic-critical tokens. The adaptive mechanism ensures that watermark strength is concentrated on tokens strongly supported by the vision content, actively guiding the model towards visual fidelity and away from potential hallucinations, particularly under high uncertainty or highly concentrated evidence weights.

In summary, our contributions are as follows:

- We propose a novel approach, AGMark, which provides cross-modal semantic guidance by identifying key vision-grounded semantics at each decoding step using attention

weights and accounting for contextual coherence in the ongoing discourse.

- AGMark determines the scale of semantic-critical tokens by jointly considering uncertainty awareness and evidence calibration, enabling adaptive vocabulary partitioning and helping to mitigate the preservation-detection trade-off.
- We conduct extensive experiments to validate AGMark in terms of text quality, visual fidelity (at least 1.7% CHAIR improvement), detectability (at least 99.36% AUC), and robustness, with a slight and acceptable increase in inference time.

2 Preliminaries

LVLM Generation. LVLMs commonly adopt a shared semantic mapping strategy, where visual representations are projected into the same embedding space as text tokens [15]. Specifically, given a model \mathcal{M} with a vocabulary \mathcal{V} of size $|\mathcal{V}|$, the visual input \mathbf{v} is first processed by a vision encoder to obtain image features. A multi-modal adapter then bridges the dimensional gap between modalities and maps these features into a visual embedding \mathcal{E}_v , which is aligned with the textual embedding matrix \mathcal{E}_t in the shared embedding space. The model subsequently generates the t -th token y_t auto-regressively by computing a distribution over \mathcal{V} :

$$l_t = \mathcal{M}(\mathbf{v}, y_{<t}), \quad p_t = \text{Softmax}(l_t), \quad (1)$$

where $y_{<t}$ denotes the textual context, $l_t \in \mathbb{R}^{|\mathcal{V}|}$ are the pre-softmax logits, and p_t is the resulting next-token distribution.

Attention Mechanism. The attention mechanism computes token relevance by projecting the hidden states from the previous layer into query Q , key K , and value V representations using projection matrices \mathbf{W}_Q , \mathbf{W}_K , and \mathbf{W}_V , respectively. The attention output at step t is defined as:

$$\text{Attention}(Q, K, V) = \mathcal{A}_t \cdot V = \text{Softmax}\left(\frac{QK^\top}{\sqrt{d_K}}\right) \cdot V, \quad (2)$$

where d_K denotes the key dimensionality, and \mathcal{A}_t^V are the attention weights used to compute contextualized representations throughout the sequence.

Logits-based Watermarking. Logits-based watermarking partitions the vocabulary into a red list \mathcal{R} and a green list \mathcal{G} according to a ratio γ (typically $|\mathcal{G}| = \gamma|\mathcal{V}|$), which is deterministically derived by hashing the prefix $y_{<t}$ together with a secret key ξ . Under this paradigm, a positive bias δ is added to the logits of tokens in \mathcal{G} , thereby increasing their sampling probability and forming a recognizable watermark pattern.

3 Methodology

We propose AGMark, a vision-aligned watermarking framework that identifies Semantic Critical Tokens to align watermark injection with visual-grounded semantics. As illustrated in Figure 2, our watermarking framework consists of two components: (A) a dynamically semantic critical weight extracting via fusing vision critical weights and context critical weights (Section 3.1); and (B) an adaptive-regulated vocabulary partition based on weight density and token entropy, that swaps high-evidence tokens into the green list (Section 3.2). This method achieves watermark injection

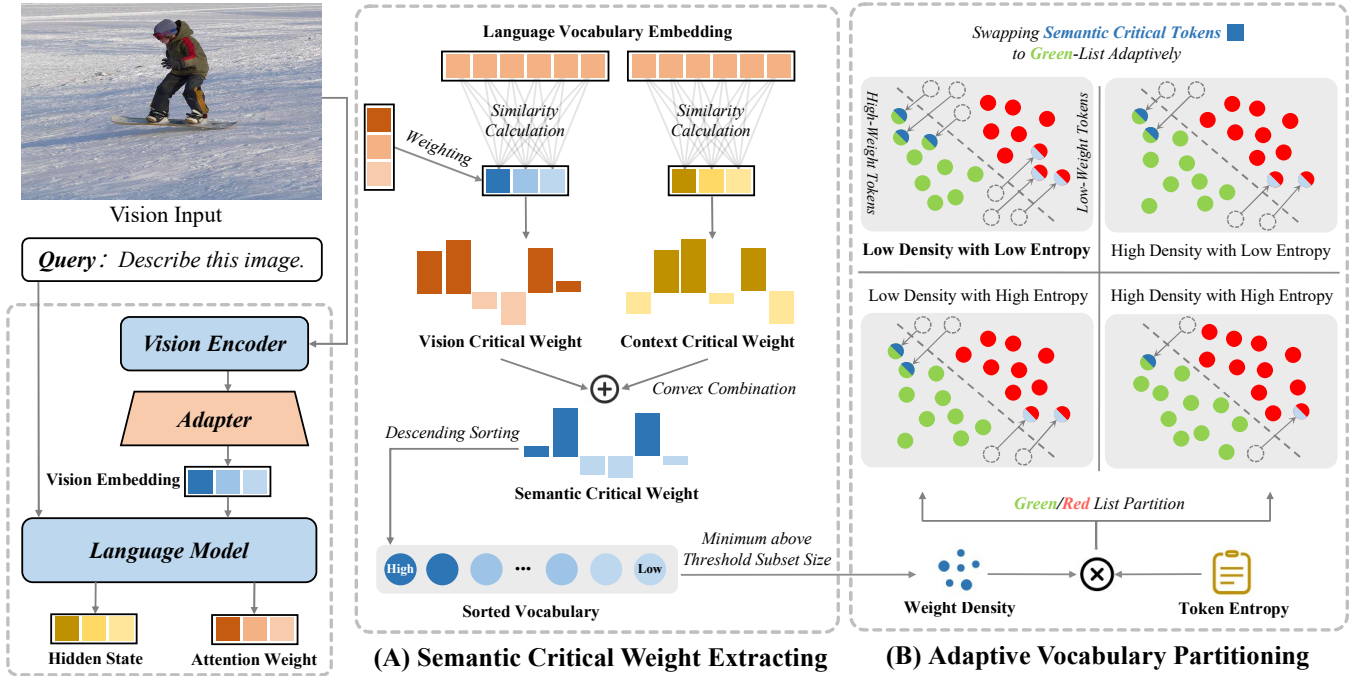


Figure 2: Overview of AGMark framework, which consists of two components: (A) Semantic Critical Weight Extracting: Dynamically extracting weight via similarity calculation to fuse vision critical weights and context critical weights. (B) Adaptive Vocabulary Partitioning: Leverages logits entropy and density of extracted weights to adaptively swap high evidence tokens into the green-list, protecting visual fidelity.

based on dynamic and precise key evidence support, yielding strong detectability with improved visual fidelity.

3.1 Semantic Critical Weight Extracting

Our first challenge is to effectively obtain *vision critical weights*. We argue that the static, one-shot computation adopted by VLA-Mark [21] is suboptimal, since the visual evidence required at each generation step may vary across decoding steps [1].

To provide appropriate and critical visually grounded tokens throughout auto-regressive decoding, we therefore compute token importance weights dynamically. The model’s attention weights \mathcal{A}_t over visual regions reflect the visual information it focuses on at generation step t , serving as a natural and informative guidance signal. In this paper, we denote the vision-token attention weights \mathcal{A}_t^v as the slice of the last-layer attention weights that corresponds to the vision token inputs v . Specifically, we derive the vision critical weights $\psi_t^v(k)$ for each vocabulary token k as:

$$\psi_t^v(k) = \mathcal{A}_t^{v\top} \cdot \frac{\mathcal{E}_v \cdot \mathcal{E}_t^{(k)}}{\|\mathcal{E}_v\| \|\mathcal{E}_t^{(k)}\|}, \quad (3)$$

where \mathcal{A}_t^v captures the model’s attention distribution over vision tokens at step t , indicating the most relevant visual evidence for the currently generated token.

However, visual saliency alone is insufficient: visual importance must be grounded in and consistent with the textual context. We use the latent representation \mathcal{E}_h [32] at the current decoding position (i.e., the last-layer hidden state) to compute a *context critical weights*

$\psi_t^c(k)$ for each vocabulary token k as:

$$\psi_t^c(k) = \frac{\mathcal{E}_h \cdot \mathcal{E}_t^{(k)}}{\|\mathcal{E}_h\| \|\mathcal{E}_t^{(k)}\|}. \quad (4)$$

To harmonize importance scores from distinct sources that may follow different distributions, we apply standardization:

$$z(x) = \frac{x - \mu}{\sigma + \epsilon}, \quad (5)$$

where μ and σ denote the mean and standard deviation of importance scores from the corresponding source, and ϵ is a small constant added to the denominator for numerical stability. This normalization maps scores to a common scale, facilitating subsequent aggregation while preserving the relative significance patterns within each source.

Finally, we derive the dynamic semantic critical weights $\psi_t(k)$ by fusing the vision critical weights $\psi_t^v(k)$ and the context critical weights $\psi_t^c(k)$ via a convex combination:

$$\psi_t(k) = \omega \cdot z(\psi_t^v(k)) + (1 - \omega) \cdot z(\psi_t^c(k)), \quad (6)$$

where $\omega \in [0, 1]$ controls the strength of visual importance or content importance. Then, we perform min–max normalization to each $\psi_t(k)$:

$$\tilde{\psi}_t(k) = \frac{\psi_t(k) - \min_{i \in \mathcal{V}} \psi_t(i)}{\max_{i \in \mathcal{V}} \psi_t(i) - \min_{i \in \mathcal{V}} \psi_t(i)}. \quad (7)$$

We sort all tokens in the vocabulary \mathcal{V} by their normalized semantic critical weights $\tilde{\psi}_t$ in descending order, yielding a prioritized

vocabulary \mathcal{V}_t^* at step t :

$$\mathcal{V}_t^* = \text{sort}_{i \in \mathcal{V}} \tilde{\psi}_t(i). \quad (8)$$

The tokens in the top portion of \mathcal{V}_t^* are referred to as *semantic critical tokens*.

Building on the above pipeline, we assign each vocabulary token k a bounded, normalized semantic critical weight $\tilde{\psi}_t(k) \in [0, 1]$, which quantifies the degree to which the current generation depends on that token. It is worth noting that this module introduces only a small number of matrix operations, resulting in a slight and acceptable increase in computational overhead. We report a detailed comparison of inference latency in Appendix B.

3.2 Adaptive Vocabulary Partitioning

Next, guided jointly by **uncertainty awareness** (token entropy) and **evidence calibration** (weight density), we dynamically determine the proportion of semantic critical tokens to be protected at the current generation step t , enabling adaptive vocabulary partitioning.

LVLMs infer the probability value p_t of the next token based on the given multi-model input, as shown in Equation 1. Specifically, at each generation step t , we measure the token entropy \mathcal{H}_t [24]:

$$\mathcal{H}_t = - \sum_{i=1}^{\mathcal{V}} p_t^{(i)} \log p_t^{(i)}. \quad (9)$$

The normalized entropy, which quantifies the uncertainty at each generation step, is then determined by:

$$\mathcal{H}_t^{\text{norm}} = \frac{\mathcal{H}_t}{\mathcal{H}_{\max}} = \frac{\mathcal{H}_t}{\log |\mathcal{V}|} \in [0, 1], \quad (10)$$

where \mathcal{H}_{\max} is the theoretical maximum value of entropy [21]. Entropy reflects the uncertainty of the model's current generation step, where lower entropy indicates that the predicted probability mass is concentrated on a small number of candidate tokens.

Additionally, inspired by the nucleus sampling (*top-p*) strategy [9], we characterize the distribution density of normalized semantic critical weights $\tilde{\psi}_t(i)$ by identifying a minimal high-importance subset of the vocabulary \mathcal{V} , thereby suppressing long-tail candidates that are more likely to yield low-quality or off-context tokens.

Specifically, we select the minimal subset $\mathcal{S}_t \subseteq \mathcal{V}$ whose cumulative importance exceeds a predefined threshold τ :

$$\mathcal{S}_t = \arg \min_{\mathcal{S} \subseteq \mathcal{V}_t^*} \left\{ |\mathcal{S}| : \sum_{i \in \mathcal{S}} \tilde{\psi}_t(i) \geq \tau \right\}. \quad (11)$$

Then, we define the weight density value ρ_t as the fraction of tokens contained in this subset:

$$\rho_t = \frac{|\mathcal{S}_t|}{|\mathcal{V}|} \in (0, 1]. \quad (12)$$

Based on the normalized entropy $\mathcal{H}_t^{\text{norm}}$ and weight density value ρ_t , we calculate the semantic critical tokens ratio η_t :

$$\eta_t = \alpha \cdot \rho_t \cdot (1 - \mathcal{H}_t^{\text{norm}}), \quad (13)$$

where the ratio α controls the base semantic critical tokens proportion. We derive the semantic critical tokens set $\mathcal{C}_t \subseteq \mathcal{V}_t^*$ based on η_t :

$$\mathcal{C}_t = \text{Top}_{\lceil \eta_t |\mathcal{V}| \rceil}(\mathcal{V}_t^*) = (\mathcal{V}_t^{*(1)}, \dots, \mathcal{V}_t^{*(\lceil \eta_t |\mathcal{V}| \rceil)}). \quad (14)$$

Then, we swap $\mathcal{A}_t = \mathcal{C}_t \cap \mathcal{R}_t$ into green by removing the $|\mathcal{A}_t|$ least-semantic critical weight tokens $\mathcal{B}_t \subseteq \mathcal{G}_t$:

$$\begin{aligned} \mathcal{G}_t &\leftarrow (\mathcal{G}_t \setminus \mathcal{B}_t) \cup \mathcal{A}_t, \\ \mathcal{R}_t &\leftarrow (\mathcal{R}_t \setminus \mathcal{A}_t) \cup \mathcal{B}_t, \end{aligned} \quad (15)$$

optionally gating the swap by a margin threshold and a per-step cap to avoid oscillation.

The watermarked probability distribution is computed following the logits-based paradigm [11], which adds a positive bias δ to the logits of tokens in \mathcal{G} , thereby increasing their sampling probability:

$$\hat{p}_t^{(k)} = \begin{cases} \frac{\exp(l_t^{(k)} + \delta)}{\sum_{i \in \mathcal{R}_t} \exp(l_t^{(i)}) + \sum_{i \in \mathcal{G}_t} \exp(l_t^{(i)} + \delta)}, & k \in \mathcal{G}_t, \\ \frac{\exp(l_t^{(k)})}{\sum_{i \in \mathcal{R}_t} \exp(l_t^{(i)}) + \sum_{i \in \mathcal{G}_t} \exp(l_t^{(i)} + \delta)}, & k \in \mathcal{R}_t. \end{cases} \quad (16)$$

Here, $\hat{p}_t^{(k)}$ denotes the watermarked probability of sampling token k at step t .

We expand the coverage of semantic critical tokens in low-entropy and dispersed weight distribution scenarios, thereby preserving the fidelity of the generated text. In other cases, the coverage of semantic critical tokens is adaptively reduced to varying degrees to enhance robustness. This dual-signal design aims to balance the trade-off between watermark embedding strength and generation quality.

4 Experimental Setup

Models and Datasets. We assess our method on three mainstream 8B LVLMs: Llava-Next-Llama3 [20], Qwen3-VL [25], and InternVL-3.5 [27]. Performance is evaluated using AMBER [26] and MSCOCO [18] datasets following prior studies [21, 35].

Evaluation Metrics. Our evaluation spans detectability performance (AUC and Accuracy), visual consistency (CHAIR [26]), text quality, and robustness against five types of attack [12, 21], which are altering text through word insertion, deletion, synonym substitution, paraphrasing, and translation. Text quality is assessed in terms of linguistic quality (Perplexity [24] and BLEU [23]) and semantic alignment (BertScore [34] and STS [2]).

Baselines. We compare our approach against five representative model watermarking baselines: KGW [11], SynthID [6], IE [7], MorphMark [29], and VLA-Mark [21]. These methods are selected for their strong emphasis on detection accuracy and text quality. Notably, VLA-Mark is specifically designed for LVLMs. Most implementations are based on the MarkLLM [22] repository.

More relevant details are reported in Appendix A.

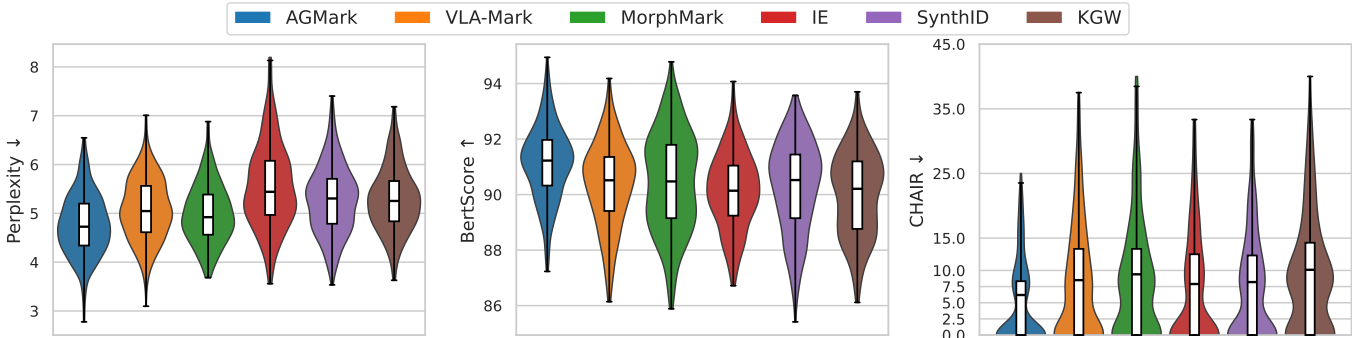
5 Results and Analysis

5.1 Main Results

Table 1 provides a detailed performance comparison of AGMark with several baseline methods across three LVLMs. The results empirically validate our primary hypothesis: While vision-agnostic watermarking mechanisms degrade generation quality, our proposing dynamically semantic critical tokens actively preserves and enhances them with maintaining detectability.

Table 1: Performance comparison in metrics AUC \uparrow , Accuracy (ACC) \uparrow , Perplexity (PPL) \downarrow , BLEU \uparrow , BertScore (BertS) \uparrow , and STS \uparrow . Bold values indicate the best performance among all methods, while underlined indicate the second best.

Model	Method	AMBER						MS COCO					
		AUC	ACC	PPL	BLEU	BertS	STS	AUC	ACC	PPL	BLEU	BertS	STS
Llava-Next	KGW	99.99	99.75	5.29	22.88	90.00	89.43	99.93	<u>98.50</u>	5.81	24.72	89.35	87.75
	SynthID	99.91	98.50	5.29	25.93	90.28	89.79	99.88	<u>98.50</u>	5.33	<u>26.37</u>	<u>90.28</u>	<u>89.87</u>
	IE	99.58	97.38	5.56	22.37	90.11	89.64	99.78	98.88	5.58	20.52	89.74	88.39
	MorphMark	99.67	97.38	<u>4.98</u>	<u>26.92</u>	<u>90.44</u>	90.07	99.75	97.75	<u>5.07</u>	25.62	90.24	89.53
	VLA-Mark	99.13	96.38	5.07	25.98	90.34	<u>90.12</u>	99.68	98.13	5.22	20.66	89.53	87.63
	AGMark (Ours)	99.91	99.50	4.80	31.88	91.14	91.85	99.91	98.88	4.95	29.86	90.76	90.51
Qwen3-VL	KGW	99.46	96.25	<u>5.83</u>	27.66	90.74	92.54	99.74	98.00	5.88	27.28	90.73	92.34
	SynthID	99.12	95.88	6.32	26.60	90.71	92.33	99.77	<u>98.00</u>	6.70	24.80	90.41	91.42
	IE	99.11	96.00	6.03	27.98	90.93	92.32	<u>99.78</u>	98.25	6.26	24.87	90.39	91.65
	MorphMark	99.27	95.75	5.81	28.87	90.93	92.93	99.64	97.25	<u>5.87</u>	28.21	90.81	92.43
	VLA-Mark	99.05	96.00	5.96	<u>31.12</u>	<u>91.40</u>	<u>93.72</u>	99.69	97.32	6.04	<u>31.10</u>	<u>91.22</u>	<u>92.91</u>
	AGMark (Ours)	99.36	96.22	<u>5.83</u>	31.88	91.46	93.99	99.82	97.88	5.85	31.95	91.45	93.81
InternVL-3.5	KGW	<u>99.57</u>	97.63	4.64	25.99	90.16	90.67	99.65	97.63	4.62	27.78	90.25	90.59
	SynthID	99.69	96.96	4.65	<u>27.27</u>	90.21	90.89	99.49	97.25	4.60	<u>28.38</u>	90.34	90.11
	IE	99.19	97.00	<u>4.52</u>	20.82	88.75	87.12	99.59	97.38	<u>4.54</u>	23.50	89.48	88.33
	MorphMark	99.56	97.38	4.56	27.20	<u>90.31</u>	90.81	99.68	97.63	4.56	27.57	90.32	90.56
	VLA-Mark	99.23	97.00	4.72	25.00	90.17	<u>91.03</u>	99.58	<u>96.75</u>	4.55	27.86	<u>90.42</u>	90.44
	AGMark (Ours)	99.57	97.50	4.50	27.45	90.40	91.12	99.65	97.85	4.53	30.88	91.08	91.74

**Figure 3: Violin plots show the sample-wise performance distribution including Perplexity (Left), BertScore (Middle), and CHAIR (Right). For Perplexity and BertScore, the overlaid box plots indicate the median. For CHAIR, however, the box plot shows the mean, since the large number of zero values for AGMark and IE would otherwise yield a median of 0.**

In terms of text quality, AGMark achieves the best performance in the vast majority of settings. For instance, on the Llava-Next backbone evaluated using AMBER dataset, it significantly outperforms the second-best method, MorphMark, in linguistic quality. Specifically, AGMark reduces perplexity by 0.18 (4.80 vs. 4.98) and improves BLEU by 4.96% (31.88% vs. 26.92%). Notably, AGMark is the only method that exceeds 91 on both semantic alignment metrics. Crucially, these improvements do not come at the cost of detectability. **Regarding detectability**, AGMark achieves an AUC above 99.36% and an accuracy above 96.22% across three models and two datasets. Notably, AGMark’s watermark detection performance AUC consistently ranks among the top two methods, indicating strong detection reliability. This confirms that embedding

visual evidence into the watermarking process effectively aligns the generated text with visual content without compromising the watermark’s statistical detectability.

5.2 Sample-wise Performance Distribution

We report sample-level performance distributions in Figure 3 to examine variability and long-tail behaviors that are not captured by aggregate metrics. In the left panel, AGMark shows a lower median perplexity than other baselines, with the lowest minimum and maximum. In the middle panel, AGMark achieves a higher median BertScore. MorphMark attains a slightly higher maximum, but also exhibits a much lower minimum. These results suggest that AGMark better preserves the original model’s language distribution,

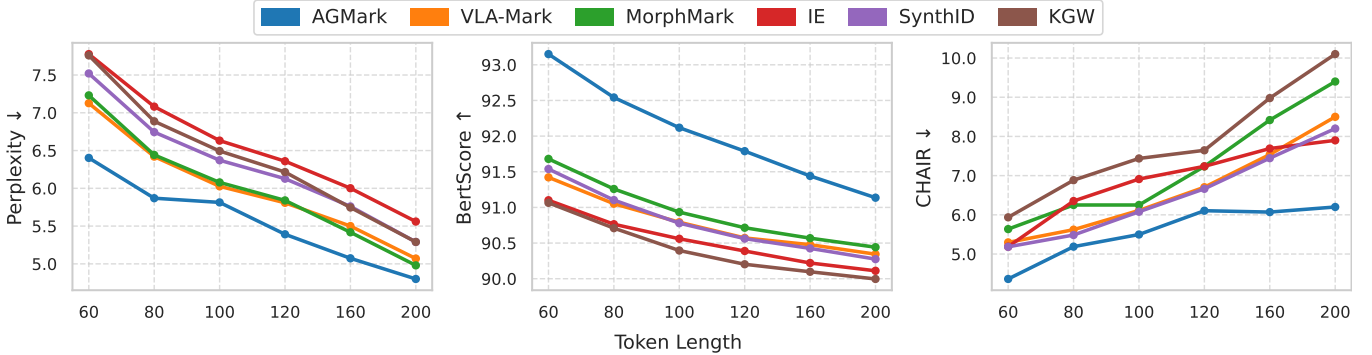


Figure 4: Line charts depict length-wise performance retention across response token lengths ranging from 60 to 200 tokens, evaluated using three metrics: Perplexity (Left), BertScore (Middle), and CHAIR (Right).

improving linguistic quality and semantic alignment. In the right panel, AGMark, IE, and SynthID are the top three methods with the lowest probability of hallucination (CHAIR). AGMark achieves the lowest mean (6.2% vs. 7.9% and 8.2%) and also the lowest maximum value, indicating better performance in both average and worst-case settings. This strong hallucination reduction suggests that AGMark effectively improves visual grounding and alignment. This demonstrates the broad applicability of our method: by dynamically and accurately identifying semantically critical tokens, AGMark not only achieves strong average performance but also avoids severe performance degradation when handling challenging samples.

5.3 Length-wise Performance Maintenance

We further analyze the impact of watermarking on text quality and visual fidelity across varying generation lengths, as shown in Figure 4. As the generation length increases, all methods exhibit rising perplexity and CHAIR scores, accompanied by a decline in BertScore, indicating that semantic drift becomes unavoidable under longer generation horizons when watermarking is applied. Beyond their generally inferior performance, some baseline methods show pronounced sensitivity to generation length, revealing weaknesses in robustness. For instance, IE attains the second-best visual-semantic alignment at 200 tokens, yet drops to second-worst rank in the 80–100 token range. In contrast, AGMark consistently maintains superior text quality and visual consistency. Notably, in the range of 120–200 tokens, AGMark demonstrates an exceptionally low rate of hallucination increase. By dynamically allocating and preserving semantically critical tokens, we minimize distortions in fluency and coherence, thereby enabling more accurate generation in the later stages.

5.4 Hyperparameter Analysis

As shown in Table 2, we investigate the impact of three critical hyperparameters in AGMark, including the fusion-strength controller ω , the base proportion of semantic-critical tokens α , and the predefined threshold τ . Hyperparameters α and τ present a clear trade-off between detectability (AUC and Accuracy) and generation quality (CHAIR, Perplexity, and BertScore), whereas the effect of ω is non-monotonic.

Table 2: The hyperparameter analysis about Llava-Next on the AMBER dataset. The results demonstrate a trade-off between detectability and visual fidelity. **Bold** values indicate the best performance among all methods.

ω	0.30	0.40	0.50*	0.60
AUC	100.00	99.99	99.91	99.94
Accuracy	99.88	99.38	99.50	99.25
CHAIR ↓	6.70	5.60	6.20	6.80
Perplexity ↓	5.17	4.87	4.80	4.82
BertScore	90.32	90.67	91.14	91.35
α	0.23	0.25	0.27*	0.29
AUC	99.97	99.94	99.91	99.85
Accuracy	99.38	99.50	99.50	98.88
CHAIR ↓	7.20	7.20	6.20	5.90
Perplexity ↓	4.82	4.79	4.80	4.78
BertScore	90.95	91.03	91.14	91.27
τ	0.90	0.95	0.98*	0.99
AUC	99.98	99.95	99.91	99.87
Accuracy	99.50	99.38	99.50	99.00
CHAIR ↓	7.60	7.70	6.20	5.80
Perplexity ↓	4.80	4.79	4.80	4.82
BertScore	90.83	91.04	91.14	91.22

Increasing α and τ consistently improves generation quality and reduces hallucinations. For example, when $\alpha = 0.29$, Perplexity and CHAIR decrease to 4.78 and 5.90%, respectively. This trend supports our design rationale. Larger α and τ allow more semantic-critical tokens to bypass random red-list exclusion, thereby protecting key content from watermark-induced perturbations and preserving generation quality. However, this protection reduces the effective space available for watermark signaling, which can weaken detectability.

In contrast, the influence of ω is non-monotonic, suggesting that careful tuning is necessary to balance visual guidance and contextual appropriateness. When ω is too small or too large, the importance weighting becomes dominated by a single modality

Table 3: Ablation study comparing the full AGMark algorithm to its variants lacking specific components. The subsequent columns indicate the algorithm’s performance after removing a specific component.

Ablation	Full	Weight Extracting			Vocabulary Partitioning		
		w/o Attention	w/o Vision	w/o Context	w/o Entropy	w/o Density	FixedScale
CHAIR ↓	6.20	8.50 _{+2.30}	7.90 _{+1.70}	7.40 _{+1.20}	7.60 _{+1.40}	8.10 _{+1.90}	8.40 _{+2.20}
Perplexity ↓	4.80	5.17 _{+0.37}	5.68 _{+0.88}	5.80 _{+1.00}	4.92 _{+0.12}	4.86 _{+0.06}	5.18 _{+0.38}
BLEU	31.88	29.63 _{-2.25}	18.25 _{-13.63}	17.94 _{-13.94}	28.11 _{-3.77}	28.65 _{-3.23}	27.63 _{-4.25}
BertScore	91.14	90.75 _{-0.39}	89.44 _{-1.70}	89.36 _{-1.78}	90.66 _{-0.48}	90.73 _{-0.41}	90.41 _{-0.73}
STS	91.85	90.47 _{-1.38}	88.20 _{-3.65}	88.05 _{-3.80}	90.50 _{-1.35}	90.63 _{-1.22}	89.99 _{-1.86}

and performance degrades. For instance, at $\omega = 0.30$ and $\omega = 0.60$, Perplexity increases to 5.17 and 4.82, indicating reduced fluency. Additionally, Relying solely on visual similarity can misidentify visual neighbors as key entities, while relying only on contextual signals can induce grounding drift in long sequences [14]. Consistent with this, hallucinations increase at extreme settings. CHAIR rises to 6.70% when $\omega = 0.30$, and it reaches 6.80% when $\omega = 0.60$. These results indicate that visual relevance and contextual consistency should be jointly considered in the decision process, which aligns with prior work [3].

However, the results also highlight that excessive values for either parameter compromise detection performance. Over-prioritizing semantic tokens or over-prioritizing publicly salient visual cues disrupts the statistical randomness required for the watermark detector, and leading to a decline in detectability efficiency. (e.g., Accuracy drops to 98.88% and 99.25% when $\alpha = 0.29$ and $\omega = 0.60$, respectively). Consequently, we identify the configuration of $\omega = 0.50$, $\alpha = 0.27$, and $\tau = 0.98$ as the optimal equilibrium.

5.5 Ablation Study

We validate the architectural effectiveness of our framework: The strategy for semantic critical weight extraction (Section 3.1) and the structural necessity of our adaptive components (Section 3.2). We construct several variants of AGMark by removing these components. For weight extracting component, we completely remove the attention-guiding to obtain *w/o Attention*, the vision critical weight to obtain *w/o Vision* ($\omega = 0.00$), and the context critical weight to obtain *w/o Context* ($\omega = 1.00$). For adaptive vocabulary partitioning component, we completely remove token entropy or weight density to obtain *w/o Entropy* and *w/o Density*. In addition, we obtain *FixedScale* by removing the adaptive vocabulary partitioning module and using a fixed scale for semantic critical tokens.

The results in Table 3 validates the critical roles of individual components in AGMark’s design and reveal some critical insights: **(1) Necessity of dynamic and dual-aspect weight extraction:** Removing any component leads to a consistent degradation across all metrics. In particular, ablating attention-guiding causes the most severe loss in vision–language semantic fidelity (a 2.30% drop), highlighting the importance of dynamically providing appropriate visual evidence at each generation step. The visual critical weighting anchors the output to visual semantics, but it can overlook narrative structure and relational plausibility. In contrast, the context critical weighting helps maintain a coherent narrative trajectory and

logical consistency, compensating for this limitation. For example, it recognizes that “waves crashing onto the shore” is correct, whereas “waves crashing onto the waves” is nonsensical, even if “waves” is visually salient evidence. **(2) Adaptive vocabulary partitioning contribution:** Ablating uncertainty awareness primarily degrades textual quality. Removing evidence calibration disrupts vision–language semantic alignment, and removing both leads to an even more pronounced performance drop. These results confirm that applying a fixed protected-token budget without accounting for model uncertainty and the distribution of semantic-critical weights can introduce erroneous markings under high-entropy states. In contrast, our adaptive mechanism effectively mitigates this risk.

5.6 Robustness against Attacks

To assess the resilience of our watermark, we evaluate AGMark against five standard text-space attacks: random word insertion, deletion, synonym substitution, paraphrasing, and translation.

Figure 5 presents the ROC curves and AUC metrics, illustrating AGMark’s superior resilience, maintaining high detectability under all attacks. Specifically, AGMark achieves an AUC of 88.61% under paraphrasing attacks, which yields the largest AUC drop of 11.28% among all attack settings. For the other attack types, the AUC drop is at most 0.87% under synonym attacks. In contrast, VLA-Mark, MorphMark, and IE suffer AUC drops of 3.34%, 2.08%, and 3.55% under synonym attacks, and drops of 26.36%, 16.46%, and 13.25% under paraphrasing attacks, respectively. Moreover, AGMark outperforms KGW under paraphrasing attacks and remains competitive under the other attack types, demonstrating strong robustness to watermark removal. We attribute these improvements to dynamic extraction of semantically salient cues and adaptive vocabulary partitioning, which keep the detector anchored to key evidence and preserve detectability even under substantial lexical and structural shifts.

6 Related Work

6.1 Watermarking

Mainstream model watermarking methods predominantly focus on unimodal text generation [21], and can be broadly categorized into two paradigms: logits-based and sampling-based [28, 32].

Logits-based watermarking methods modify the token probability distribution over the vocabulary during decoding. The pioneering KGW [11] method uses a hash key to divide the vocabulary into red and green lists, favoring green tokens in the output. IE [7]

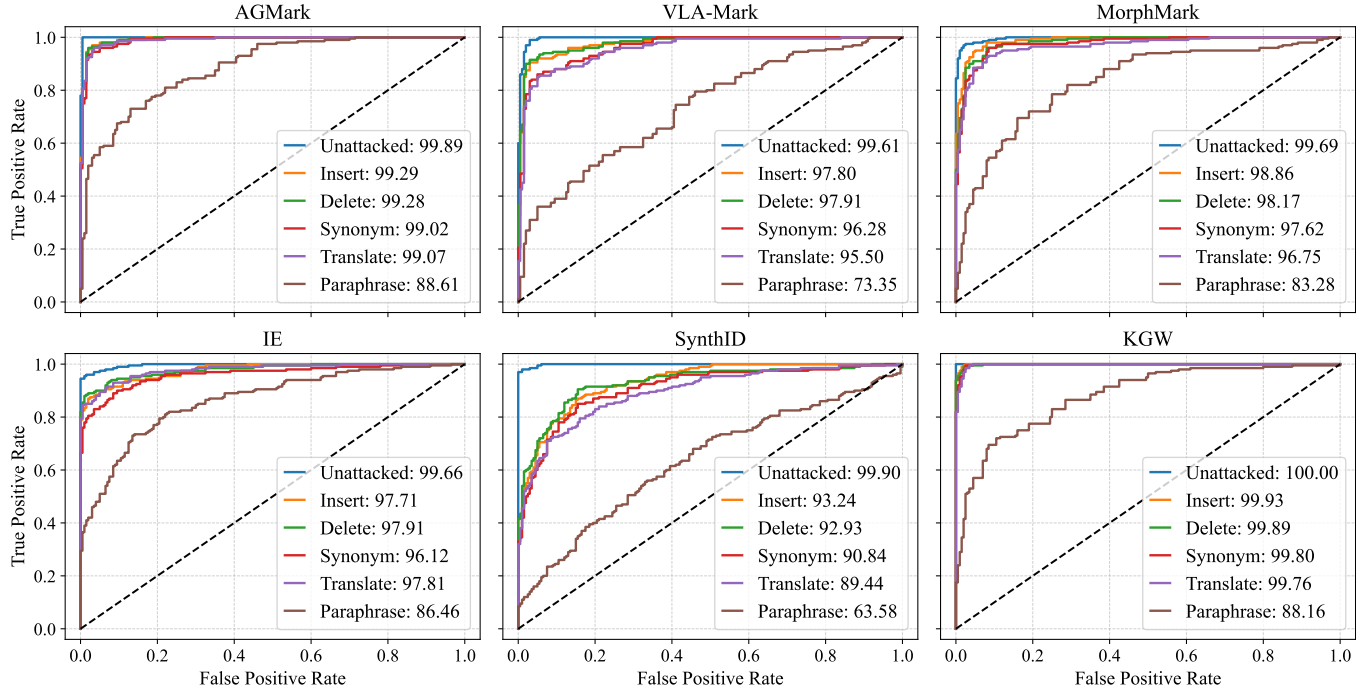


Figure 5: AUC matrix for six watermarking methods under various attack scenarios, with AUC values reported in parentheses. Smaller differences between pre-attack and post-attack AUC indicate stronger robustness against the corresponding attacks. The relative performance drop comparison as shown in Appendix C.

trains an entropy navigator that reduces the injection intensity as the number of green tokens increases under low entropy conditions. MorkphMark [29] demonstrates that the sum of probabilities of green tokens in the watermark plays a crucial role in balancing the trade-off between injection intensity and text quality, determining the injection intensity based on the probability of green tokens. Meanwhile, *sampling-based* watermarking methods alter the sampling process by leveraging pseudorandom sequences to guide token selection. Christ et al. [5] propose a binary sampling method for LLMs based on pseudo-random number generation, though it is unsuitable for real-world LLMs. SynthID [6] introduces a tournament-based strategy for token generation. In contrast, current research in sampling-based watermarking is limited, indicating room for advancement [19].

Additionally, two recent logits-based watermarking methods for LLMs, VLA-Mark [21] and VISA-Mark [35], both follow a common design: they compute visual-importance weights and balance watermark strength via an entropy-sensitive mechanism to guide watermark injection. However, their static, global, one-shot importance estimation limits the ability to identify semantic-critical tokens in a more fine-grained and accurate manner. Our proposed AGMark leverages attention-guided visual relevance to identify the most pertinent visual evidence and incorporates contextual coherence to dynamically and precisely protect semantic-critical tokens at each decoding step, thereby achieving a balanced trade-off between watermark detectability and generation quality.

6.2 Watermark Removal Attacks

Watermarks face the threat of being removed by malicious attackers in real-world applications. Attacks against watermarking algorithms can be broadly categorized into text manipulations and informed watermark attacks.

Text manipulations involve traditional NLP techniques to straightforward text manipulations, such as word deletion, substitution, or insertion [12]. Translation is also a common form of attack, and watermarks lack consistency in their detectability across different languages [8]. By altering the word-level structure of the text, these methods attempt to distort or eliminate the watermark. In contrast, document-level attacks introduce more substantial changes to content and discourse structure, with paraphrasing being the most prevalent approach [19]. Paraphrasing attacks can be carried out either manually [11] or using large language models [4]. More broadly, paraphrasing includes both monolingual rewriting and its cross-lingual variant realized through translation (optionally followed by back-translation), which has been shown to effectively degrade watermark detectability [12, 19].

A representative example of *informed watermark attacks* is watermark stealing [10, 30], where an attacker queries the watermarking algorithm to reverse-engineer or approximate the watermarking rule, estimate the watermark distribution of the target model, and infer whether each token conforms to the watermark constraint via a large number of carefully designed prefix queries conditioned on the context. However, such methods typically assume essentially

unlimited access to the watermarked model, which limits their practicality in real-world settings.

7 Conclusion

In this paper, we present AGMark, a vision-language aligned dynamic watermarking framework that harmonizes intellectual property protection with cross-modal semantic fidelity. By combining attention-guided extraction of dynamic semantic-critical weights with an adaptive vocabulary partitioning strategy that incorporates uncertainty awareness and evidence calibration, our method addresses the long-standing trade-off between watermark detectability and visual-semantic consistency in existing approaches. Empirical results demonstrate that AGMark achieves clear advantages, delivering strong detectability and high robustness while also improving overall visual fidelity and overall text quality. This work establishes a novel paradigm for watermarking in LVLMs, and we hope AGMark will help promote the responsible use of artificial intelligence technologies.

References

- [1] Peter Anderson, Xiaodong He, Chris Buehler, Damien Teney, Mark Johnson, Stephen Gould, and Lei Zhang. 2018. Bottom-up and top-down attention for image captioning and visual question answering. In *Proceedings of the IEEE conference on computer vision and pattern recognition*. 6077–6086.
- [2] Daniel Cer, Mona Diab, Eneko Agirre, Iñigo Lopez-Gazpio, and Lucia Specia. 2017. SemEval-2017 Task 1: Semantic Textual Similarity Multilingual and Crosslingual Focused Evaluation. In *Proceedings of the 11th International Workshop on Semantic Evaluation (SemEval-2017)*. Steven Bethard, Marine Carpuat, Marianna Apidianaki, Saif M. Mohammad, Daniel Cer, and David Jurgens (Eds.). Association for Computational Linguistics, Vancouver, Canada, 1–14. doi:10.18653/v1/S17-2001
- [3] Jiahe Chen, Jiaying He, Qian Shao, Qiyuan Chen, Jiahe Ying, Hongxiao Xu, Jintai Chen, Jianwei Zheng, and Jian Wu. 2025. Mitigating Hallucination of Large Vision-Language Models via Dynamic Logits Calibration. *arXiv preprint arXiv:2506.21509* (2025).
- [4] Yixin Cheng, Hongcheng Guo, Yangming Li, and Leonid Sigal. 2025. Revealing Weaknesses in Text Watermarking Through Self-Information Rewrite Attacks. In *Forty-second International Conference on Machine Learning*.
- [5] Miranda Christ, Sam Gunn, and Or Zamir. 2024. Undetectable watermarks for language models. In *The Thirty Seventh Annual Conference on Learning Theory*. PMLR, 1125–1139.
- [6] Sumanth Dathathri, Abigail See, Sumedh Ghaisas, Po-Sen Huang, Rob McAdam, Johannes Welbl, Vandana Bachani, Alex Kaskasoli, Robert Stanforth, Tatiana Matejovicova, et al. 2024. Scalable watermarking for identifying large language model outputs. *Nature* 634, 8035 (2024), 818–823.
- [7] Tianle Gu, Zongqi Wang, Kexin Huang, Yuanqi Yao, Xiangliang Zhang, Yujun Yang, and Xiuying Chen. 2025. Invisible Entropy: Towards Safe and Efficient Low-Entropy LLM Watermarking. In *Proceedings of the 2025 Conference on Empirical Methods in Natural Language Processing*. Christos Christodoulopoulos, Tanmoy Chakraborty, Carolyn Rose, and Violet Peng (Eds.). Association for Computational Linguistics, Suzhou, China, 6716–6733. doi:10.18653/v1/2025.emnlp-main.341
- [8] Zhiwei He, Binglin Zhou, Hongkun Hao, Aiwei Liu, Xing Wang, Zhaopeng Tu, Zhusheng Zhang, and Rui Wang. 2024. Can Watermarks Survive Translation? On the Cross-lingual Consistency of Text Watermark for Large Language Models. In *Proceedings of the 62nd Annual Meeting of the Association for Computational Linguistics (Volume 1: Long Papers)*. 4115–4129.
- [9] Ari Holtzman, Jan Buys, Li Du, Maxwell Forbes, and Yejin Choi. 2020. The Curious Case of Neural Text Degeneration. In *International Conference on Learning Representations*.
- [10] Nikola Jovanović, Robin Staab, and Martin Vechev. 2024. Watermark stealing in large language models. In *Proceedings of the 41st International Conference on Machine Learning*. 22570–22593.
- [11] John Kirchenbauer, Jonas Geiping, Yuxin Wen, Jonathan Katz, Ian Miers, and Tom Goldstein. 2023. A watermark for large language models. In *International Conference on Machine Learning*. PMLR, 17061–17084.
- [12] Gregory Kang Ruey Lau, Xinyuan Niu, Hieu Dao, Jiangwei Chen, Chuan-Sheng Foo, and Bryan Kian Hsiang Low. 2024. Waterfall: Scalable Framework for Robust Text Watermarking and Provenance for LLMs. In *Proceedings of the 2024 Conference on Empirical Methods in Natural Language Processing*. Yaser Al-Onaizan, Mohit Bansal, and Yun-Nung Chen (Eds.). Association for Computational Linguistics, Miami, Florida, USA, 20432–20466. doi:10.18653/v1/2024.emnlp-main.1138
- [13] Taehyun Lee, Seokhee Hong, Jaewoo Ahn, Ilgee Hong, Hwaran Lee, Sangdoo Yun, Jamin Shin, and Gunhee Kim. 2024. Who wrote this code? watermarking for code generation. In *Proceedings of the 62nd Annual Meeting of the Association for Computational Linguistics (Volume 1: Long Papers)*. 4890–4911.
- [14] Jiaming Li, Jiacheng Zhang, Zequan Jie, Lin Ma, and Guanbin Li. 2025. Mitigating hallucination for large vision language model by inter-modality correlation calibration decoding. *arXiv preprint arXiv:2501.01926* (2025).
- [15] Wenyan Li, Raphael Tang, Chengzu Li, Caiqi Zhang, Ivan Vulić, and Anders Søgaard. 2025. Lost in Embeddings: Information Loss in Vision-Language Models. In *Findings of the Association for Computational Linguistics: EMNLP 2025*. Christos Christodoulopoulos, Tanmoy Chakraborty, Carolyn Rose, and Violet Peng (Eds.). Association for Computational Linguistics, Suzhou, China, 22676–22693. doi:10.18653/v1/2025.findings-emnlp.1235
- [16] Yue Li, Xin Yi, Dongsheng Shi, Yongyi Cui, Gerard de Melo, and Linlin Wang. 2025. From Injection to Defense: Constructing Edit-Based Fingerprints for Large Language Models. *arXiv preprint arXiv:2509.03122* (2025).
- [17] Yue Li, Xin Yi, Dongsheng Shi, Gerard De Melo, Xiaoling Wang, and Linlin Wang. 2025. Hierarchical Safety Realignment: Lightweight Restoration of Safety in Pruned Large Vision-Language Models. In *Findings of the Association for Computational Linguistics: ACL 2025*. Wanxiang Che, Joyce Nabende, Ekaterina Shutova, and Mohammad Taher Pilehvar (Eds.). Association for Computational Linguistics, Vienna, Austria, 7600–7612. doi:10.18653/v1/2025.findings-acl.394
- [18] Tsung-Yi Lin, Michael Maire, Serge Belongie, James Hays, Pietro Perona, Deva Ramanan, Piotr Dollár, and C Lawrence Zitnick. 2014. Microsoft coco: Common objects in context. In *European conference on computer vision*. Springer, 740–755.
- [19] Aiwei Liu, Leyi Pan, Yijian Lu, Jingjing Li, Xuming Hu, Xi Zhang, Lijie Wen, Irwin King, Hui Xiong, and Philip Yu. 2024. A survey of text watermarking in the era of large language models. *Comput. Surveys* 57, 2 (2024), 1–36.
- [20] Haotian Liu, Chunyuan Li, Yuheng Li, Bo Li, Yuanhan Zhang, Sheng Shen, and Yong Jae Lee. 2024. LLaVA-NeXT: Improved reasoning, OCR, and world knowledge. <https://llava-vl.github.io/blog/2024-01-30-llava-next/>
- [21] Shuliang Liu, Zheng Qi, Jesse Jiaxi Xu, Yibo Yan, Junyan Zhang, He Geng, Aiwei Liu, Peijie Jiang, Jia Liu, Yik-Cheung Tam, and Xuming Hu. 2025. VLA-Mark: A cross modal watermark for large vision-language alignment models. In *Proceedings of the 2025 Conference on Empirical Methods in Natural Language Processing*. Christos Christodoulopoulos, Tanmoy Chakraborty, Carolyn Rose, and Violet Peng (Eds.). Association for Computational Linguistics, Suzhou, China, 26409–26427. doi:10.18653/v1/2025.emnlp-main.1342
- [22] Leyi Pan, Aiwei Liu, Zhiwei He, Zitian Gao, Guandong Zhao, Yijian Lu, Binglin Zhou, Shuliang Liu, Xuming Hu, Lijie Wen, et al. 2024. MarkLLM: An Open-Source Toolkit for LLM Watermarking. In *Proceedings of the 2024 Conference on Empirical Methods in Natural Language Processing: System Demonstrations*. 61–71.
- [23] Kishore Papineni, Salim Roukos, Todd Ward, and Wei-Jing Zhu. 2002. Bleu: a Method for Automatic Evaluation of Machine Translation. In *Proceedings of the 40th Annual Meeting of the Association for Computational Linguistics*. Pierre Isabelle, Eugene Charniak, and Dekang Lin (Eds.). Association for Computational Linguistics, Philadelphia, Pennsylvania, USA, 311–318. doi:10.3115/1073083.1073135
- [24] Claude E Shannon. 1948. A mathematical theory of communication. *The Bell system technical journal* 27, 3 (1948), 379–423.
- [25] Qwen Team. 2025. Qwen3 Technical Report. *arXiv:2505.09388 [cs.CL]* <https://arxiv.org/abs/2505.09388>
- [26] Junyang Wang, Yuhang Wang, Guohai Xu, Jing Zhang, Yukai Gu, Haitao Jia, Jiaqi Wang, Haiyang Xu, Ming Yan, Ji Zhang, et al. 2023. Amber: An llm-free multi-dimensional benchmark for milms hallucination evaluation. *arXiv preprint arXiv:2311.07397* (2023).
- [27] Weiyang Wang, Zhangwei Gao, Lixin Gu, Hengjun Pu, Long Cui, Xingguang Wei, Zhaoyang Liu, Linglin Jing, Shenglong Ye, Jie Shao, et al. 2025. InternV3.5: Advancing open-source multimodal models in versatility, reasoning, and efficiency. *arXiv preprint arXiv:2508.18265* (2025).
- [28] Yidan Wang, Yubing Ren, Yanan Cao, and Binxing Fang. 2025. From Trade-off to Synergy: A Versatile Symbiotic Watermarking Framework for Large Language Models. In *Proceedings of the 63rd Annual Meeting of the Association for Computational Linguistics (Volume 1: Long Papers)*. Wanxiang Che, Joyce Nabende, Ekaterina Shutova, and Mohammad Taher Pilehvar (Eds.). Association for Computational Linguistics, Vienna, Austria, 10306–10322. doi:10.18653/v1/2025.acl-long.509
- [29] Zongqi Wang, Tianle Gu, Baoyuan Wu, and Yujiu Yang. 2025. MorphMark: Flexible Adaptive Watermarking for Large Language Models. In *Proceedings of the 63rd Annual Meeting of the Association for Computational Linguistics (Volume 1: Long Papers)*. Wanxiang Che, Joyce Nabende, Ekaterina Shutova, and Mohammad Taher Pilehvar (Eds.). Association for Computational Linguistics, Vienna, Austria, 4842–4860. doi:10.18653/v1/2025.acl-long.240
- [30] Qilong Wu and Varun Chandrasekaran. 2024. Bypassing LLM Watermarks with Color-Aware Substitutions. In *Proceedings of the 62nd Annual Meeting of the Association for Computational Linguistics*. 1–14.

Association for Computational Linguistics (Volume 1: Long Papers). 8549–8581.

[31] Mang Ye, Xuankun Rong, Wenke Huang, Bo Du, Nenghai Yu, and Dacheng Tao. 2025. A survey of safety on large vision-language models: Attacks, defenses and evaluations. *arXiv preprint arXiv:2502.14881* (2025).

[32] Xin Yi, Yue Li, Dongsheng Shi, Linlin Wang, Xiaoling Wang, and Liang He. 2026. Latent-space adversarial training with post-aware calibration for defending large language models against jailbreaks attacks. *Expert Systems with Applications* 296 (2026), 129101. doi:10.1016/j.eswa.2025.129101

[33] Xin Yi, Yue Li, Shunfai Zheng, Linlin Wang, Xiaoling Wang, and Liang He. 2025. Unified attacks to large language model watermarks: Spoofing and scrubbing in unauthorized knowledge distillation. *Knowledge-Based Systems* 329 (2025), 114295. doi:10.1016/j.knosys.2025.114295

[34] Tianyi Zhang, Varsha Kishore, Felix Wu, Kilian Q Weinberger, and Yoav Artzi. 2020. BERTScore: Evaluating Text Generation with BERT. In *International Conference on Learning Representations*.

[35] Qi Zheng, Shuliang Liu, Yu Huang, Sihang Jia, Jungang Li, Lyuhao Chen, Junhao Chen, Hanqian Li, Aiwei Liu, Yibo Yan, et al. 2026. A Visual Semantic Adaptive Watermark grounded by Prefix-Tuning for Large Vision-Language Model. *arXiv preprint arXiv:2601.07291* (2026).

A Experimental Details

Environments. Experiments are conducted on a system equipped with six NVIDIA GeForce RTX 3090 GPUs with 24 GB of memory each, and two Quadro RTX 8000 GPUs with 48 GB of memory each.

Hyperparameter Settings. For a fair comparison, we standardize the hyperparameters across methods:

- For the main hyperparameters, we follow the default settings of the MarkLLM [22] repository.
- We set $\gamma = 0.5$ to keep the size of the green vocabulary consistent across different watermarking methods.
- To ensure a controlled comparison and avoid imbalanced watermark strength, we tune the watermark injection strength (i.e., δ) to achieve an AUC of at least 99%.

Seed. We use seed 42 as the default seed for all experiments.

B Efficiency

Table 4 shows the end-to-end generation latency for 10 images and 200 tokens on three LVLMs. Our AGMark adds only a small overhead over existing text-only watermarking methods. While AGMark introduces a moderate latency increase compared to light-weight baselines like KGW, the additional overhead is manageable (e.g., approx. +0.41s on Qwen3-VL relative to the unwatermarked baseline). This trade-off is justified by the significant gains in generation quality.

C Relative Performance Drop under Attacks

These attacks are applied to the first 200 samples. Table 5 quantifies AGMark’s resilience through relative AUC drops under six attack scenarios.

Table 4: Inference latency (average generation time cost in seconds) for different watermarking methods across LVLMs.

Model	AGMark (Ours)	VLA-Mark	MorphMark	IE	SynthID	KGW	unwatermarked
Llava-Next	13.6288	13.5321	12.9452	15.0930	13.2575	12.6046	12.8765
InternVL-3.5	18.2620	18.1217	17.4910	19.6789	18.7429	17.3230	17.1905
Qwen3-VL	21.8015	21.5862	21.6214	22.9254	22.7037	21.5226	21.3882

Table 5: Relative performance drop (%) from unattacked baseline under adversarial attacks. Bold values indicate the best performance among all methods, while underlined indicate the second best.

Method	Unattacked	Insert	Delete	Synonym	Translate	Paraphrase
KGW	0.00 (100.00)	0.07 (99.93)	0.11 (99.89)	0.20 (99.80)	0.24 (99.76)	<u>11.84 (88.16)</u>
SynthID	0.00 (99.90)	6.66 (93.24)	6.97 (92.93)	9.06 (90.84)	10.46 (89.44)	<u>36.32 (63.58)</u>
IE	0.00 (99.66)	1.96 (97.71)	1.76 (97.91)	3.55 (96.12)	1.86 (97.81)	<u>13.25 (86.46)</u>
MorphMark	0.00 (99.69)	0.83 (98.86)	1.52 (98.17)	2.08 (97.62)	2.95 (96.75)	<u>16.46 (83.28)</u>
VLA-Mark	0.00 (99.61)	1.82 (97.80)	1.71 (97.91)	3.34 (96.28)	4.13 (95.50)	<u>26.36 (73.35)</u>
AGMark (Ours)	0.00 (99.89)	<u>0.70 (99.29)</u>	<u>0.71 (99.28)</u>	<u>0.87 (99.02)</u>	<u>0.82 (99.07)</u>	11.28 (88.61)